

Exciton dynamics probed in carbon nanotube suspensions with narrow diameter distribution

Tobias Hertel^{*1,2}, Zipeng Zhu¹, Jared Crochet¹, Claiborne McPheeters³,
Hendrik Ulbricht⁴, and Daniel Resasco⁵

¹ Department of Physics and Astronomy, Vanderbilt University, Nashville, TN, USA

² Institute for Nanoscale Science and Engineering, Vanderbilt University, Nashville, TN, USA

³ Department of Electrical Engineering, University of California San Diego, San Diego, CA, USA

⁴ Institute for Experimental Physics, University of Vienna, Vienna, Austria

⁵ School of Chemical Engineering and Materials Science, University of Oklahoma, Norman, OK, USA

Received 25 April 2006, accepted 9 August 2006

Published online 2 October 2006

PACS 71.35.-y, 78.47.+p, 78.67.Ch

We report on a pump–probe study of CoMoCAT nanotube suspensions with narrow chirality distribution. Visible pump pulses and a white light continuum are used for resonant excitation of the strongest dipole allowed E_{22} subband exciton in the semiconducting (6, 5) tube and for broadband probe of the resulting spectral transients between 1300 nm and 480 nm, respectively. Transient spectra show signatures of both photobleaching (PB) and photoabsorption (PA) with practically identical decay- but slightly different rise-times. The experiments reveal that apparent variations of decay rates at different wavelengths do not reflect dynamics of different relaxation processes but are a consequence of the superposition of PB and blue-shifted PA response.

© 2006 WILEY-VCH Verlag GmbH & Co. KGaA, Weinheim

1 Introduction

The spectroscopy of semiconducting carbon nanotubes has witnessed breathtaking progress over the last 4 years, since photoluminescence from isolated semiconducting SWNTs was first reported by O’Connell et al. [1]. This work facilitated the identification of diameter and chirality of specific tube types by photoluminescence excitation spectroscopy and absorption spectroscopy [2–5]. In addition, the electronic states observed in absorption and emission spectra were found to be excitonic in character [6, 7] with extraordinary high exciton binding energies of several hundred meV [8–13]. The dynamics of excited states have likewise received considerable interest [14–20] owing to the relevance of energy relaxation processes for the performance of nano- and optoelectronic devices [21–23].

Many aspects of excited state dynamics in semiconducting SWNTs, such as their wavelength dependence as well as the assignment and interpretation of bleaching and photoabsorption transients, however, remain controversial. Transitions from $E_{11}(1u)$ to higher exciton and free carrier like states as well as excited state line broadening have been discussed as possible origin for the observed dynamics [24–26]. Here we present an investigation of exciton dynamics in chirality enriched nanotube samples using femtosecond time resolved pump–probe spectroscopy. The use of samples with high concentration of the

* Corresponding author: e-mail: tobias.hertel@vanderbilt.edu, Phone: +1 615 322-2864, Fax: +1 615 343-7263

(6, 5) tube type, in combination with resonant excitation of the respective E_{22} exciton states allows to obtain a better understanding of the spectral transients.

2 Results and discussion

2.1 Sample preparation

Nanotube suspensions are prepared from CVD synthesized CoMoCAT material [27] using surfactant aided solubilization in aqueous environment [1]. The suspensions are mixed from 1 mg of nanotube soot with 2 wt% of surfactant in 20 ml H_2O . Nanotube material, surfactant and solvent are agitated ultrasonically in an ice bath using a Branson 450 Sonifier with a tapered microtip at 30% duty cycle. Samples are then centrifuged in a Sorvall ultracentrifuge with a swinging bucket rotor for 4 hours at 30,000 g. The supernatant is decanted and used for spectroscopy.

The surfactant used in these experiments is sodium dodecylbenzene sulfonate (SDBS) [1, 28]. The density of similar, DNA suspended SWNT samples with tubes of roughly 1 nm diameter has previously been found to be $1.13 \text{ g} \times \text{cm}^{-3}$ [29]. Since the density of H_2O solvent is significantly smaller than $1.13 \text{ g} \times \text{cm}^{-3}$, tubes in these suspensions must have a high mobility to remain suspended in the presence of strong centrifugal forces. Suspensions are thus likely to be characterized by an abundance of individual tubes over larger agglomerates as well as by an abundance of short length tubes over longer ones which have lower diffusion constants.

Samples prepared in such a manner have been characterized by Raman- [30], absorption- and photoluminescence spectroscopy [2]. The average length of tubes in samples obtained from CoMoCat material – as determined by AFM – is around 250 nm [29]. Absorption and photoluminescence spectroscopy suggest that the most prominent semiconducting tube in these samples is the (6, 5) tube (see Fig. 2a). Analysis of linear absorption spectra allows to tentatively estimate the relative concentration of the (6, 5) tube to be around $(35 \pm 5) \text{ wt}\%$ of all semiconducting nanotubes based on the relative spectral weight of the (6, 5) tube. Recent Raman investigations conclude that the (6, 5) contribution to semiconducting tubes in CoMoCAT samples is slightly higher with about 43 wt% [30].

2.2 Setup for pump–probe spectroscopy

Pump–probe experiments are performed with a regenerative amplifier driven optical parametric amplifier (Coherent Inc., RegA 9000 and OPA 9450) at 250 kHz repetition rate. The parametric amplifier provides tuneable sub 50 fs laser pulses in the visible range of the spectrum (470 nm–730 nm) with pulse fluences of up to $0.3 \mu\text{J}$. The instrument also generates a white light continuum which can be used as broadband probe from 1.6 μm up to 420 nm. The pump beam is focused into a spectrophotometer cell with 10 mm light path using a lens of 75 mm focal length (see Fig. 1). The broadband probe beam is likewise focused into this cell using spherical 100 mm focal length reflective optics. Pump and probe beams at the focus are estimated to be 100 μm in diameter. In combination with the skew angle between pump and probe beams this gives rise to an increase of the pulse cross-correlation width of less than 30 fs. Unless noted otherwise, pulse fluences are kept below $1 \times 10^{14} \text{ cm}^{-2}$.

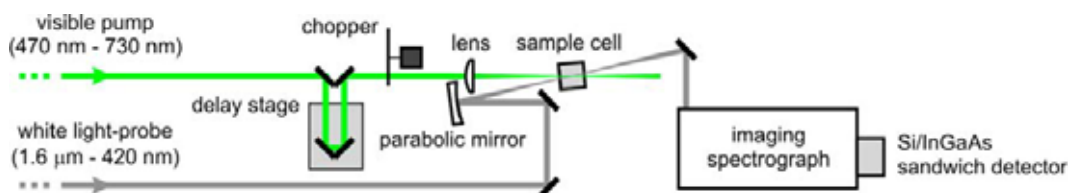


Fig. 1 (online colour at: www.pss-b.com) Schematic illustration of the experimental setup used for pump–probe spectroscopy.

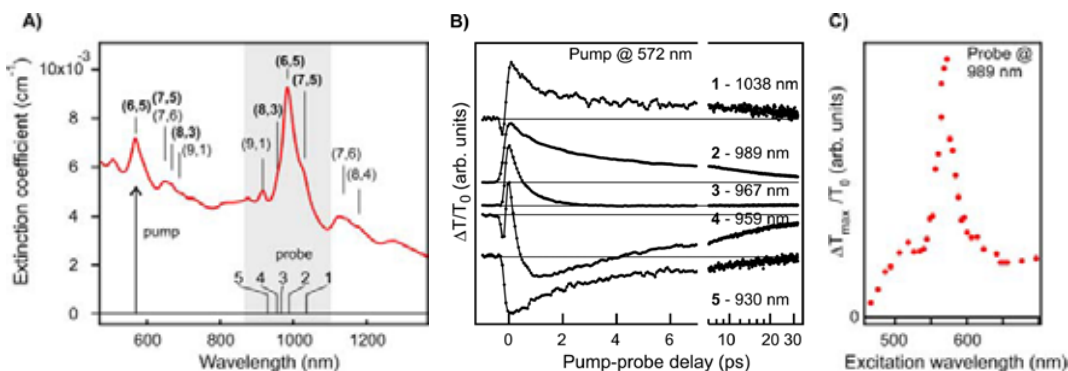


Fig. 2 (online colour at: www.pss-b.com) a) Linear absorption spectrum of a CoMoCAT@SDBS sample. b) Cross-correlations for resonant excitation of the E_{22} exciton in (6, 5) tubes at 572 nm. c) Enhancement of the $E_{11}(1u)$ transients (probed at 998 nm) for resonant excitation of the corresponding E_{22} exciton.

The pump beam delay is adjusted using a computer controlled delay stage (Physik Instrumente, PI-M521.DD) with a bi-directional reproducibility of positions of $0.1 \mu\text{m} = 0.66 \text{ fs}$. The white light probe beam is dispersed in an imaging spectrograph (Jobin Yvon, Triax 320) and detected by a thermoelectrically cooled Si/InGaAs sandwich detector. Optical transients $\Delta T/T_0$ or $\Delta I/I_0$ (differential transmission), or $\Delta\alpha$ (differential absorption) can be recorded with a sensitivity of up to 2×10^{-6} using phase sensitive detection as facilitated by chopping the pump beam, typically at 1 kHz.

At the wavelengths used in this study, photoabsorption cross sections of sp^2 hybridized polyaromatic hydrocarbon compounds on the order of $1 \times 10^{-18} \text{ cm}^2/\text{atom}$ [31, 32] lead to roughly one absorbed photon per 100 nm of tube length. The associated temperature increase of the tube lattice is on the order of 1 K or less. Power dependent measurement of optical transients confirmed that saturation occurs at significantly higher pulse fluences.

2.3 Interpretation of optical transients

Differential transmission/absorption spectroscopy measures the normalized difference of transmitted reference $I_R(\omega)$ and probe $I_P(\omega)$ beams as given by $\Delta I/I_0 = e^{-\Delta\alpha(\omega)L}$. This is related to the third order polarizability $P^{(3)}(\omega)$ and the amplitude of the probe field $E_T(\omega)$ [33]:

$$\frac{\Delta I(\omega)}{I_0(\omega)} \approx \frac{n\omega L}{\epsilon_0 c} \text{Im} \frac{P^{(3)}(\omega)}{E_T(\omega)}$$

where L is the optical path length through the probe volume with refractive index n . The time-dependent polarization is given by the evolution of the off-diagonal elements of the density matrix. Here, the off-diagonal elements ρ_{Xg} of the $E_{11}(1u)$ exciton state initially prepared by the pump beam are assumed to vanish because the state is being populated through relaxation from the E_{22} higher energy state. The optical response can then be traced back to the pump induced difference of the populations in the ground (g) and exciton (X) states ($\rho_{XX} - \rho_{gg}$) [33] without having to account for coherent effects.

When interpreting optical transients one thus needs to bear in mind that the dynamics of relaxation and repopulation of excited and ground states, respectively, may involve a number of additional states such as triplet excitons, dark excitons or trap states which are not directly observed in pump–probe spectra but which nevertheless affect the return to the ground state [12, 13]. The transients discussed in the following section thus have to be seen in the light of relaxation and repopulation dynamics. In contrast, photoluminescence quantum yields and the dynamics of the associated PL decay generally reflect the population dynamics of the photoluminescent state X [14–16].

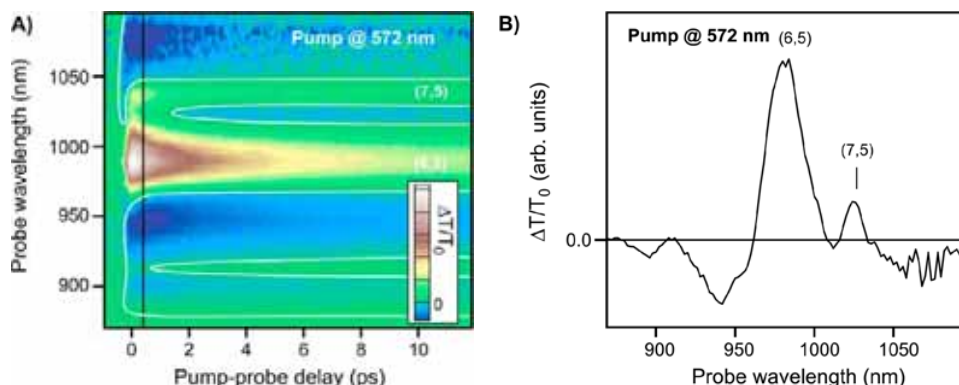


Fig. 3 (online colour at: www.pss-b.com) a) Map of optical transients in the E_{11} energy range for resonant excitation of the E_{22} transition in (6, 5) tubes. b) Transient spectrum at a small positive pump–probe delay of 0.2 ps.

3.4 Broadband probe of optical transients in the $E_{11}(1u)$ exciton range

A linear absorption spectrum of a CoMoCat-SDS sample is shown in Fig. 2a and the cross-correlations in Fig. 2b for resonant excitation of the E_{22} subband exciton of the dominant (6, 5) tube species are taken at different probe wavelengths. Pump-wavelength dependent measurements of the response at the $E_{11}(1u)$ resonance energy (989 nm) indicate that transients at this wavelength exhibit a similar enhancement as PL from the (6, 5) tube in photoluminescence excitation spectroscopy (see Fig. 2c) [34]. A more detailed reproduction of the spectral dynamics in the E_{11} range is reproduced in Fig. 3a. Similar transients have been reported by a number of groups, mostly on suspensions fabricated from HipCO material where spectra tend to be more heavily congested.

The optical transients shown in Fig. 2b exhibit photobleaching (PB) as well as photoabsorption (PA). Closer inspection of the PB at 989 nm and the PA signal at 930 nm reveals that the cross-correlations are characterized by practically identical decay behaviour. The response at 930 nm, however is characterized by a longer risetime by about 0.3 ps if compared with the 989 nm response. The seemingly complex behaviour at intermediate wavelengths, e.g. at 959 nm, can mostly be attributed to a superposition of the dynamics at 930 nm and 989 nm indicating that transients at those wavelengths are manifestations of the same relaxation processes. Further evidence for the common origin of the PB signal at 989 nm and the PA at 930 nm is provided by similar resonance behaviour of transients when the excitation energy is tuned through the E_{22} resonance as well as by similar saturation behaviour. Signals at other wavelengths in the spectrum, for example at energies smaller than the (6, 5) $E_{11}(1u)$ resonance show different resonance and saturation behaviour. This suggests that PB and PA signal contributions at the resonance itself and its high energy side, respectively can be attributed to dynamics of the resonantly excited (6, 5) tube while other signal contributions have to be attributed to dynamics in non-resonantly excited tubes. Such discrimination is generally not possible in heavily congested spectra.

Despite the similarity of PB and PA dynamics we here find that a host of cross-correlations with seemingly different character can be interpreted more or less as a simple superposition of the two processes. Examples are the rapid decay of the cross-correlation at 967 nm in Fig. 2b or the peculiar dynamics at 959 nm.

Phenomenologically the observed PB and PA transients may be interpreted as blue shift and absorption line narrowing. A blue-shift of the $E_{11}(1u)$ feature can tentatively be assigned to exciton–exciton interactions, leading to a blue-shift of the excited state with respect to the ground state absorption spectrum as observed for excited state absorption in excitonically coupled dimers. The narrowing may be

associated with spectral hole-burning through selective excitation of a spectrally slightly more confined sub-ensemble by the pump beam.

The interpretation of the mechanism underlying short and longer term dynamics is likewise complicated by the aforementioned influence of ground state repopulation on the optical transients. This becomes evident from a comparison of transients in solubilized photoluminescent (6, 5) tubes and non-photoluminescent ropes made from the same samples. The optical transients of rope and single tube samples are found to be surprisingly similar despite the at least one order of magnitude lower PL quantum yield in ropes [35]. This suggests that the initial decay of optical transients at the $E_{11}(1u)$ resonance energy reflect the population dynamics of that state only very weakly and that great care must be taken when discussing these dynamics in the context of radiative and non-radiative decay of the $E_{11}(1u)$ state. Efficient internal conversion or intersystem crossing from the E_{22} exciton to dipole forbidden states might be responsible for the weak dependence of the $E_{11}(1u)$ transients on PL quantum yields.

In summary, we have presented initial results of a femtosecond time-resolved visible pump-broadband probe study of optical transients in chirality enriched nanotube suspensions with an abundance of (6, 5) tubes. The experiments facilitate a better understanding of the complex wavelength dependence of optical transients in multidisperse samples. We can show that the seemingly complex behaviour of cross correlations at different wavelengths can be attributed to the superposition of photobleaching and blue-shifted photoabsorption with similar decay rates but a slightly delayed risetime for the PA component. This is tentatively assigned to s-dynamical blue shift and narrowing of the (6, 5) tube excited state absorption spectrum.

References

- [1] M. J. O'Connell, S. M. Bachilo, C. B. Huffman et al., *Science* **297**, 593 (2002).
- [2] S. M. Bachilo, L. Balzano, J. E. Herrera et al., *J. Am. Chem. Soc.* **125**, 11186 (2003).
- [3] A. Hagen and T. Hertel, *Nano Lett.* **3**, 383 (2003).
- [4] R. B. Weisman and S. M. Bachilo, *Nano Lett.* **3**, 1235 (2003).
- [5] S. Lebedkin, F. Hennrich, T. Skipa et al., *J. Phys. Chem. B* **107**, 1949 (2003).
- [6] T. Ando, *J. Phys. Soc. Jpn.* **66**, 1066 (1997).
- [7] H. Htoon, M. J. O'Connell, P. J. Cox et al., *Phys. Rev. Lett.* **93**, 027401 (2004).
- [8] F. Wang, G. Dukovic, L. E. Brus et al., *Science* **308**, 838 (2005).
- [9] J. Maultzsch, R. Pomraenke, S. Reich et al., *Phys. Rev. B* **72**, 241402(R) (2005).
- [10] C. D. Spataru, S. Ismail-Beigi, L. X. Benedict et al., *Appl. Phys. A, Mater. Sci. Process.* **78**, 1129 (2004).
- [11] E. Chang, G. Bussi, A. Ruini et al., *Phys. Rev. Lett.* **92**, 196401 (2004).
- [12] H. B. Zhao and S. Mazumdar, *Phys. Rev. Lett.* **93**, 157402 (2004).
- [13] V. Perebeinos, J. Tersoff, and P. Avouris, *Phys. Rev. Lett.* **92**, 257402 (2004).
- [14] Y. Z. Ma, J. Stenger, J. Zimmermann et al., *J. Chem. Phys.* **120**, 3368 (2004).
- [15] F. Wang, G. Dukovic, L. E. Brus et al., *Phys. Rev. Lett.* **92**, 177401 (2004).
- [16] A. Hagen, G. Moos, V. Talalaev et al., *Appl. Phys. A, Mater. Sci. Process.* **78**, 1137 (2004).
- [17] A. Hagen, M. Steiner, M. B. Raschke et al., *Phys. Rev. Lett.* **95**, 197401 (2005).
- [18] J. S. Lauret, C. Voisin, G. Cassaboiss et al., *Phys. Rev. Lett.* **90**, 57404 (2003).
- [19] S. Reich, M. Dworzak, A. Hoffmann et al., *Phys. Rev. B* **71**, 33402 (2005).
- [20] G. N. Ostojic, S. Zaric, J. Kono et al., *Phys. Rev. Lett.* **92**, 117402 (2004).
- [21] J. A. Misewich, R. Martel, P. Avouris et al., *Science* **300**, 783 (2003).
- [22] L. Marty, E. Adam, L. Albert et al., *Phys. Rev. Lett.* **96**, 136803 (2006).
- [23] Z. H. Chen, J. Appenzeller, Y. M. Lin et al., *Science* **311**, 1735 (2006).
- [24] O. J. Korovyanko, C. X. Sheng, Z. V. Vardeny et al., *Phys. Rev. Lett.* **92**, 17403 (2004).
- [25] G. N. Ostojic, S. Zaric, J. Kono et al., *Phys. Rev. Lett.* **94**, 97401 (2005).
- [26] Y. Z. Ma, L. Valkunas, S. M. Bachilo et al., *J. Phys. Chem. B* **109**, 15671 (2005).
- [27] D. E. Resasco, W. E. Alvarez, F. Pompeo et al., *J. Nanoparticle Res.* **4**, 131 (2002).
- [28] T. Hertel, A. Hagen, V. Talalaev et al., *Nano Lett.* **5**, 511 (2005).
- [29] M. S. Arnold, S. I. Stupp, and M. C. Hersam, *Nano Lett.* **5**, 713 (2005).
- [30] A. Jorio, A. P. Santos, H. B. Ribeiro et al., *Phys. Rev. B* **72**, 75207 (2005).

- [31] G. Mallocci, G. Mulas, and C. Joblin, *Astron. Astrophys.* **426**, 105 (2004).
- [32] M. F. Islam, D. E. Milkie, C. L. Kane et al., *Phys. Rev. Lett.* **94**, 019901 (2005).
- [33] M. Joffre, in: *Femtosecond Laser Pulses*, edited by C. Rullière (Springer, Berlin, 1998), p. 261.
- [34] S. M. Bachilo, M. S. Strano, C. Kittrell et al., *Science* **298**, 2361 (2002).
- [35] T. Hertel, Z. Zhu, and J. Crochet, to be submitted.